



Inelastic x-ray scattering study of superconducting $\text{SmFeAsO}_{1-x}\text{F}_x$ single crystals: Evidence for strong momentum-dependent doping-induced renormalizations of optical phonons

M. Le Tacon,^{1,2} T. R. Forrest,³ Ch. Rüegg,³ A. Bosak,¹ A. C. Walters,^{1,3} R. Mittal,⁴ H. M. Rønnow,⁵ N. D. Zhigadlo,⁶ S. Katrych,⁶ J. Karpinski,⁶ J. P. Hill,⁷ M. Krisch,¹ and D. F. McMorrow³

¹European Synchrotron Radiation Facility, BP 220, F-38043 Grenoble Cedex, France

²Max-Planck-Institut für Festkörperforschung, Heisenbergstraße 1, D-70569 Stuttgart, Germany

³London Centre for Nanotechnology and Department of Physics and Astronomy, University College London, London WC1E 6BT, United Kingdom

⁴Solid State Physics Division, Bhabha Atomic Research Centre, Trombay, Mumbai 400 085, India

⁵Laboratory for Quantum Magnetism, Ecole Polytechnique Fédérale de Lausanne, CH-1015 Lausanne, Switzerland

⁶Laboratory for Solid State Physics, ETH Zürich, CH-8093 Zürich, Switzerland

⁷Department of Condensed Matter Physics and Materials Science, Brookhaven National Laboratory, Upton, New York 11973, USA

(Received 12 October 2009; revised manuscript received 27 November 2009; published 21 December 2009)

We report inelastic x-ray scattering experiments on the lattice dynamics in SmFeAsO and superconducting $\text{SmFeAsO}_{0.60}\text{F}_{0.35}$ single crystals. Particular attention was paid to the dispersions along the $[100]$ direction of three optical modes close to 23 meV, polarized out of the FeAs planes. Remarkably, two of these modes are strongly renormalized upon fluorine doping. These results provide significant insight into the energy and momentum dependence of the coupling of the lattice to the electron system and underline the importance of spin-phonon coupling in the superconducting iron pnictides.

DOI: [10.1103/PhysRevB.80.220504](https://doi.org/10.1103/PhysRevB.80.220504)

PACS number(s): 74.25.Kc, 63.20.-e, 74.25.Gz, 78.70.Ck

The recent discovery of superconductivity in FeAs-based compounds has stimulated considerable interest.¹ To date three distinct families of FeAs-based superconductors with respective formulas $X\text{FeAs}$ ($X=\text{Li}$ or Na), $M\text{Fe}_2\text{As}_2$ ($M=\text{Ca}, \text{Ba}, \text{Sr}$), and REFeAsO (where RE is a rare-earth metal)—the so-called “111’s,” “122’s,” and “1111’s”—have been identified. Among them, the last family has the highest values of the superconducting transition temperature T_c : depending on the lanthanide, T_c can be as high as 55 K.² The high value of T_c and early DFT calculations³ initially appeared to support the notion of an exotic mechanism for superconductivity in these materials. However, recent experiments have established that the role of phonons in the electron coupling cannot be totally ignored. In particular, the observation of large Fe isotope effects⁴ and the fact that the Fe-As configuration is intimately related to T_c (Ref. 5) and to the magnetic state of the iron sublattice^{6,7} show that the lattice is actively involved in this problem. In addition, substantial deviations have been found between the experimentally observed phonon density of states (PDOS) and *ab initio* calculations,⁸ suggesting that these calculations do not capture all the relevant physics. A spin-polarized calculation is, for example, required to obtain good agreement with the experimental phonon dispersion in the case of undoped CaFe_2As_2 , even above the magnetic ordering temperature T_N .⁹ Furthermore, it was recently demonstrated that zone-center Raman active phonons are strongly renormalized at T_N in $\text{Ba}_{1-x}\text{K}_x\text{Fe}_2\text{As}_2$ (Ref. 10) and $\text{Ba}(\text{Fe}_{1-x}\text{Co}_x)_2\text{As}_2$.¹¹ These results all highlight the role of spin-phonon coupling in iron pnictides.

In previous experiments on $\text{NdFeAsO}_{1-x}\text{F}_x$ powders, an unexpected signature of the doping in the PDOS was discovered.¹² In particular, it was found that even at room temperature, at least one of the three phonon branches located around 23 meV softens on doping. All the three modes

are polarized out of the (Fe,As) planes, parallel to the c axis, and involve motions of either the As or Fe ions. At least one of the modes couples directly to the magnetic iron sublattice.^{7,13}

Here, we utilize inelastic x-ray scattering (IXS) to investigate the phonon dispersions of SmFeAsO and superconducting $\text{SmFeAsO}_{0.60}\text{F}_{0.35}$ single crystals, with particular emphasis on these three modes. We find an unexpectedly strong doping-induced renormalization of the 21 meV (As,Sm) and 26 meV (Fe,O) modes. In addition, this renormalization displays a nontrivial momentum dependence. Taken together, these results provide significant insight into the evolution with doping of the energy and momentum dependence of the coupling between the lattice and the spin degrees of freedom and suggest that the spin-phonon coupling is of key importance.

High-quality single crystals of SmFeAsO and $\text{SmFeAsO}_{0.60}\text{F}_{0.35}$ were grown as described elsewhere.^{14,15} Our magnetization measurements on SmFeAsO using a superconducting quantum interference device show magnetic ordering at $T_N=130$ K, and the superconducting transition in the nominally doped $\text{SmFeAsO}_{0.60}\text{F}_{0.35}$ takes place at $T_c=53$ K. Contrary to 122 pnictide single crystals, the samples available are of very small size (about $100 \times 100 \times 20 \mu\text{m}^3$ for the ones we used in this experiment) and consequently their phonon dispersions can only be investigated using IXS. The IXS experiments were carried out on beamline ID28 at the European Synchrotron Radiation Facility, with a photon energy of 21.747 keV and an energy resolution of 2.0 meV. The x-ray beam was focused down to $50 \times 40 \mu\text{m}^2$. Rocking curves of 0.5° were measured on the (004) reflection, indicating a low c -axis mosaicity. Phonon intensities are proportional to $(\mathbf{Q} \cdot \boldsymbol{\sigma}_n)^2$,¹⁶ with $\boldsymbol{\sigma}_n$ being the eigenvectors of the modes and $\mathbf{Q}=(Q_a \ Q_b \ Q_c)$ being the total momentum transfer, defined here with respect to the tetragonal unit cell (a

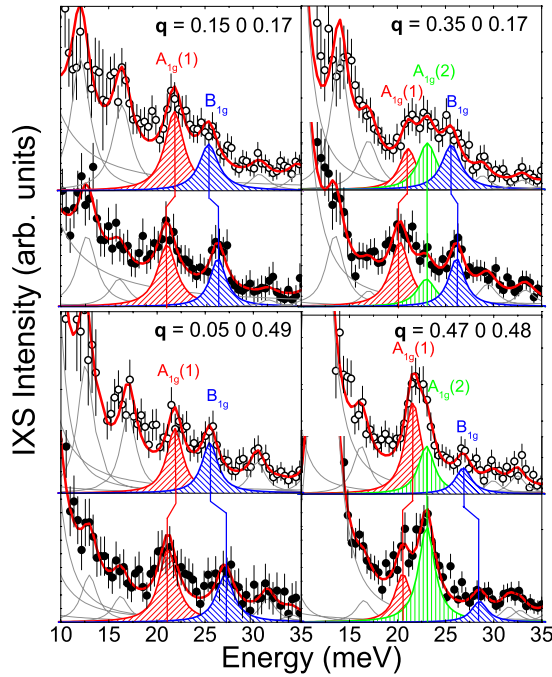


FIG. 1. (Color online) Doping dependence of the IXS spectra of $\text{SmFeAs}(\text{O}_{1-x}\text{F}_x)$ for four \mathbf{Q} positions (open circles: SmFeAsO ; full circles: $\text{SmFeAsO}_{0.60}\text{F}_{0.35}$). The red line is the result of the total fit, and the thin gray lines are the individual phonons. The three phonon lines around 23 meV have been highlighted. Clear energy shifts, with opposite signs, are observed in the 21 and 26 meV modes.

$=b=3.936$ Å, $c=8.485$ Å for SmFeAsO and $a=b=3.931$ Å, $c=8.472$ Å for $\text{SmFeAsO}_{0.60}\text{F}_{0.35}$). In what follows we also use $\mathbf{q}=(q_a q_b q_c)$ for the reduced momentum transfer. We therefore carried out our measurements in zones with the largest Q_c component possible to maximize the intensity for the three c -axis polarized phonons we were interested in. All results were obtained at room temperature.

Figure 1 shows the main results of our study. Here, phonon spectra for SmFeAsO and $\text{SmFeAsO}_{0.60}\text{F}_{0.35}$ are presented close to the $(1\ 0\ 12)$ Γ point at four different momentum transfers, corresponding to $(q_a\ 0\ 0.17)$ (upper panel) and approximately $(q_a\ 0\ 0.5)$ (lower panel). Three features are observed around 23 meV. Two of them display a clear doping dependence. The phonon located around 21 meV systematically softens on going from the undoped to the doped compound, while the phonon close to 26 meV hardens. The third feature, located around 23 meV, is only observed at large q_a and shows essentially no doping dependence, except at $\mathbf{q}=(0.45\ 0\ 0.17)$ where it is softened by about 0.5 meV (not shown here).

The spectra were analyzed by fitting to a series of Lorentzians, as shown in Figs. 1 and 2. With the exception of the elastic line, fitting of the data to resolution limited peaks gave rather poor results, and slightly broader line shapes (2.2–2.5 meV) were used. Similar broadening has also been reported in the case of CaFe_2As_2 .¹⁷ Such broadening is potentially interesting, but widths could not be extracted with enough confidence due to the low statistics. We thus focus here on the energy of the phonons, which are extracted reliably.

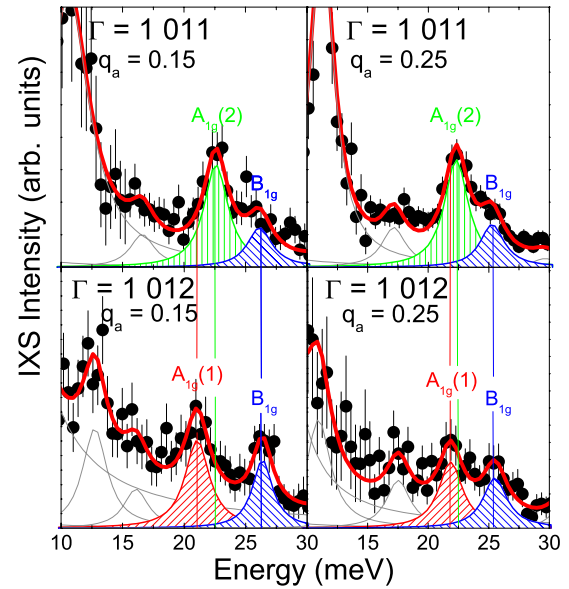


FIG. 2. (Color online) Experimental IXS spectra of $\text{SmFeAsO}_{0.60}\text{F}_{0.35}$ for $\mathbf{q}=(0.15\ 0\ 0.17)$ (left) and $\mathbf{q}=(0.25\ 0\ 0.17)$ (right) in two different Brillouin zones: $\Gamma=(1\ 0\ 11)$ (upper panel) and $\Gamma=(1\ 0\ 12)$ (lower panel). The red line is the result of the total fit, and the thin gray lines the individual phonons. The three phonon lines around 23 meV have been highlighted.

To allow unambiguous assignment of the three modes around 23 meV, we mapped out their dispersion. Only two are visible at small q_a for measurements carried out close to the $(1\ 0\ 12)$ Γ point, so we also recorded several spectra close to the $(1\ 0\ 11)$ Γ point for the $\text{SmFeAsO}_{0.60}\text{F}_{0.35}$ sample. This is illustrated in Fig. 2, where we show energy scans at $q_a=0.15$ and 0.25 in the two different zones [$\Gamma=(1\ 0\ 12)$ and $\Gamma=(1\ 0\ 11)$]. The 26 meV mode is present in both zones, while the mode at 23 meV [21 meV] is seen only for measurements carried out from $\Gamma=(1\ 0\ 11)$ [$\Gamma=(1\ 0\ 12)$].

The dispersion of these modes along the $(q_a\ 0\ 0)$ direction for the two compounds is summarized in Fig. 3. The theoretical dispersion for LaFeAsO from Ref. 18 is also shown, and we have added the Raman (stars) and infrared (IR, triangle) data obtained on SmFeAsO in Refs. 19 and 20. Our data extrapolate well to these zone-center measurements, allowing us to assign our experimental points to the three c -axis polarized Raman modes: the 21 meV mode is assigned to the in-phase A_{1g} (As,Sm) mode [red, labeled $A_{1g}(1)$ in Figs. 1–4], the 23 meV mode to the out-of-phase A_{1g} (As,Sm) mode [green, $A_{1g}(2)$], and the 26 meV mode to the B_{1g} (Fe,O) mode (blue). In addition to the transverse acoustic branch at low energy, we note the presence of other branches, one around 12 meV that could be assigned to the IR-active c -axis polarized (Sm,Fe,As) A_{2u} mode, and another around 17 meV, whose energy seems to correspond to the in-plane polarized E_g mode. However, their precise identifications remain challenging due to the large discrepancies between the IXS intensities predicted by the DFT calculations and the experimental spectra. Some of these modes also seem to display a doping dependence, and we also note that

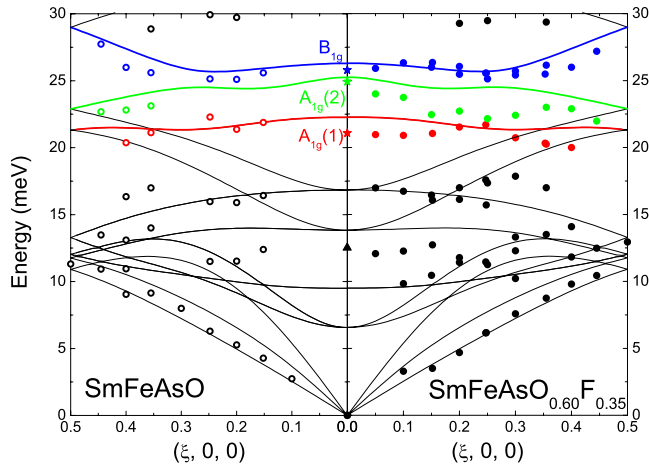


FIG. 3. (Color online) Experimental phonon dispersion along the $(q_a 0 0)$ direction of the parent SmFeAsO (left panel) and superconducting SmFeAsO_{0.60}F_{0.35} (right panel), at room temperature. Data points with $|q_c| \leq 0.17$ were included (the “doubling” of some points at a given q_a is due to a slightly different q_c in the two measurements). Error bars derived from the fitting are smaller than the data points. Full lines correspond to the theoretical dispersion of LaFeAsO from Ref. 18 and may be considered as a guide to the eye. The three c -axis polarized Raman active modes (see text) have been highlighted. Note that further modes extend up to 55 meV in these materials (not shown).

their relative intensities are strongly renormalized, indicating additional doping-induced changes in the lattice dynamics. A complete study of these phenomena is beyond the scope of this Rapid Communication and requires further investigation.

From this assignment and the comparison of doped and undoped spectra shown in Fig. 1, it follows that the two modes that display the strongest doping dependence are the in-phase A_{1g} (As,Sm) mode at 21 meV and the B_{1g} (Fe,O) mode at 26 meV. We have exploited the eight analyzers available on beamline ID28 to map the \mathbf{q} dependence of the amplitude of the doping-induced shifts of these modes in the $(q_a 0 q_c)$ plane. The results are plotted in Fig. 4. Remarkably, we find that the doping-induced renormalization of these modes varies strongly with momentum transfer. The maximum amplitude of the softening of the A_{1g} mode in the $(q_a 0 q_c)$ plane is found to be 1.2 meV close to $\mathbf{q} = (0.3 0 0.3)$, while the largest hardening of the B_{1g} mode is found to be 1.7 meV close to $\mathbf{q} = (0.5 0 0.5)$. We note that this doping dependence of the Fe vibration contrasts with recent nuclear resonant IXS measurements,²¹ which showed no doping dependence of the Fe partial PDOS of LaFeAsO_{1-x}F_x.

It is worth stressing that our results are not consistent with extant first-principles calculations. Early calculations based on the virtual crystal approximation suggested that doping should induce only minor changes in the phonon spectra.³ Our previous PDOS data¹² together with the present single-crystal data demonstrate the failure of such an approach to properly describe the effects of doping. More recently, F doping was explicitly taken into account in a $2 \times 2 \times 1$ supercell within a local-density approximation approach.¹⁸ The authors concluded that the doping-induced changes seen in

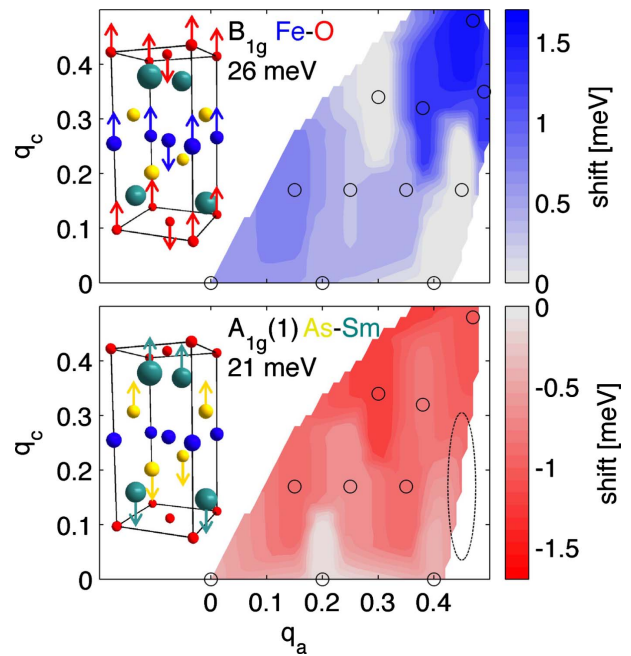


FIG. 4. (Color online) Momentum dependence of the doping-induced renormalization of the 26 meV B_{1g} (upper panel) and 21 meV in-phase A_{1g} (lower panel) modes in the $(q_a 0 q_c)$ plane. The empty circles correspond to the analyzer positions, the dashed ellipse indicates the \mathbf{q} resolution, and the white shades indicate where there are insufficient data. The insets show schematics of the respective $\mathbf{q} = \mathbf{0}$ eigenvectors, with the atoms color coded as indicated.

the PDOS (Ref. 12) were strictly related to structural relaxation. Doping was also predicted to induce hardening for the out-of-phase A_{1g} (As,Sm) and B_{1g} (Fe,O) modes and a splitting of the in-phase A_{1g} (As,Sm) mode. Experimentally, we observe a hardening of the B_{1g} mode, but see no evidence for the in-phase A_{1g} mode splitting—each feature of the undoped sample’s spectra has a one-to-one correspondence with a feature observed in the doped compound. Moreover, as emphasized earlier, only a softening of this mode is observed. Finally, for the few points where we have been able to measure the out-of-phase A_{1g} (As,Sm) phonon in both samples, no energy renormalization, or at most only a small softening is observed.

The improved agreement between experiments carried out above T_N in parent 122 compounds, and lattice dynamics calculations following the inclusion of spin polarization,⁹ indicates that magnetism is the missing ingredient in the *ab initio* calculations discussed above. In this regard, theoretical studies suggest that the magnetic ground state is intimately related to the Fe-As distance along the c axis.^{6,7} A corollary to this is that atomic motions modulating this distance, as the in-phase A_{1g} (As,Sm) mode and the B_{1g} (Fe,O) mode do, must couple to the amplitude of the Fe moments.¹³ In contrast, the out-of-phase A_{1g} (As,Sm) mode is expected to only weakly change the FeAs tetrahedra and therefore to exhibit only weak spin-phonon coupling.⁷ Indeed, this phonon shows little or no renormalization, which suggests that the effects observed here reflect a coupling of the electronic system to the lattice through this spin channel. Further, coupling

may be possible with the antiferromagnetic fluctuations known to be present in the paramagnetic phase.^{22,23}

Our data provide two important clues as to the form of this coupling. First, the opposite shift of the two magnetically active phonons is highly unusual and suggests that there may be some kind of resonance in the electronic system around 23 meV, with the bare phonons lying on either side of this resonance.²⁴ Second, the maps of the magnitude of the renormalization (Fig. 4) provide some hints of the momentum dependence of this coupling. In principle, the momentum and energy dependence of the observed renormalization could have two sources: the electron-phonon coupling, $g(\mathbf{q}, \omega)$, and the (magnetic or electronic) susceptibility, $\chi(\mathbf{q}, \omega)$. Both may evolve with doping, although in the absence of additional theoretical and experimental inputs it is difficult to resolve their respective contributions to the effects reported here (although we note that changes in the magnetic susceptibility induced by modifications of the nesting conditions with doping have been discussed²⁵). Nevertheless, it is interesting to speculate that the evolution of this coupling, the signatures of which we have observed here in the phonon spectra, may potentially play a role in the dra-

matic changes in the low-temperature ground states.

In summary, we report a strong doping dependence of the two *c*-axis polarized in-phase A_{1g} (As,Sm) and B_{1g} (Fe,O) modes in the paramagnetic state of the $\text{SmFeAs}(\text{O}_{1-x}\text{F}_x)$ iron pnictide. The doping-induced renormalizations of these two modes have opposite signs and show an unexpected momentum dependence that remains to be understood. Our results strongly suggest that phonons play an active role in the physics of iron pnictides and that both further theoretical and experimental investigations are urgently required to clarify this point. Of most relevance here, we note that it has been argued that the coupling between the in-phase A_{1g} mode and the magnetic iron sublattice could (strongly) enhance the electron-phonon coupling in the iron pnictides.¹³

This project was supported by the U.S. Department of Energy, Division of Materials Science, under Contract No. DE-AC02-98CH10886, by the Swiss National Science Foundation (NCCR MaNEP), the Royal Society, and EPSRC. The authors are grateful to J. v. d. Brink, A. Yaresko, and D. Inosov for useful conversations, and to J. Noffsinger for providing us his DFT calculation.

-
- ¹H. Takahashi, K. Igawa, K. Arii, Y. Kamihara, M. Hirano, and H. Hosono, *Nature (London)* **453**, 376 (2008).
- ²Z.-A. Ren, W. Lu, J. Yang, W. Yi, X.-L. Shen, C. Zheng, G.-C. Che, X.-L. Dong, L.-L. Sun, F. Zhou, and Z.-X. Zhao, *Chin. Phys. Lett.* **25**, 2215 (2008).
- ³L. Boeri, O. V. Dolgov, and A. A. Golubov, *Phys. Rev. Lett.* **101**, 026403 (2008).
- ⁴R. H. Liu, T. Wu, G. Wu, H. Chen, X. F. Wang, Y. L. Xie, J. J. Ying, Y. J. Yan, Q. J. Li, B. C. Shi, W. S. Chu, Z. Y. Wu, and X. H. Chen, *Nature (London)* **459**, 64 (2009).
- ⁵H. Mukuda, N. Terasaki, H. Kinouchi, M. Yashima, Y. Kitaoka, S. Suzuki, S. Miyasaka, S. Tajima, K. Miyazawa, P. Shirage, H. Kito, H. Eisaki, and A. Iyo, *J. Phys. Soc. Jpn.* **77**, 093704 (2008).
- ⁶Z. P. Yin, S. Lebegue, M. J. Han, B. P. Neal, S. Y. Savrasov, and W. E. Pickett, *Phys. Rev. Lett.* **101**, 047001 (2008).
- ⁷T. Yildirim, *Physica C* **469**, 425 (2009).
- ⁸T. Fukuda, A. Q. R. Baron, S.-i. Shamoto, M. Ishikado, H. Nakamura, M. Machida, H. Uchiyama, S. Tsutsui, A. Iyo, H. Kito, J. Mizuki, M. Arai, H. Eisaki, and H. Hosono, *J. Phys. Soc. Jpn.* **77**, 103715 (2008).
- ⁹S. E. Hahn, Y. Lee, N. Ni, P. C. Canfield, A. I. Goldman, R. J. McQueeney, B. N. Harmon, A. Alatas, B. M. Leu, E. E. Alp, D. Y. Chung, I. S. Todorov, and M. G. Kanatzidis, *Phys. Rev. B* **79**, 220511(R) (2009).
- ¹⁰M. Rahlenbeck, G. L. Sun, D. L. Sun, C. T. Lin, B. Keimer, and C. Ulrich, *Phys. Rev. B* **80**, 064509 (2009).
- ¹¹L. Chauvière, Y. Gallais, M. Cazayous, A. Sacuto, M. A. Measson, D. Colson, and A. Forget, *Phys. Rev. B* **80**, 094504 (2009).
- ¹²M. Le Tacon, M. Krisch, A. Bosak, J. W. G. Bos, and S. Margadonna, *Phys. Rev. B* **78**, 140505(R) (2008).
- ¹³F. Yndurain and J. M. Soler, *Phys. Rev. B* **79**, 134506 (2009).
- ¹⁴N. D. Zhigadlo, S. Katrych, Z. Bukowski, S. Weyeneth, R. Puzniak, and J. Karpinski, *J. Phys.: Condens. Matter* **20**, 342202 (2008).
- ¹⁵J. Karpinski, N. D. Zhigadlo, S. Katrych, Z. Bukowski, P. Moll, S. Weyeneth, H. Keller, R. Puzniak, M. Tortello, D. Daghero, R. Gonnelli, I. Maggio-Aprile, Y. Fasano, Ø. Fischer, K. Rogacki, and B. Batlogg, *Physica C* **469**, 370 (2009).
- ¹⁶E. Burkel, *Rep. Prog. Phys.* **63**, 171 (2000).
- ¹⁷R. Mittal, L. Pintschovius, D. Lamago, R. Heid, K. P. Bohnen, D. Reznik, S. L. Chaplot, Y. Su, N. Kumar, S. K. Dhar, A. Thamizhavel, and T. Brueckel, *Phys. Rev. Lett.* **102**, 217001 (2009).
- ¹⁸J. Noffsinger, S. G. Louie, M. L. Cohen, and F. Giustino, *Phys. Rev. Lett.* **102**, 147003 (2009).
- ¹⁹V. G. Hadjiev, M. N. Iliev, K. Sasmal, Y. Y. Sun, and C. W. Chu, *Phys. Rev. B* **77**, 220505(R) (2008).
- ²⁰C. Marini, C. Mirri, G. Profeta, S. Lupi, D. Di Castro, R. Sopracase, P. Postorino, P. Calvani, A. Perucchi, S. Massidda, G. M. Tropeano, M. Putti, A. Martinelli, A. Palenzona, and P. Dore, *EPL* **84**, 67013 (2008).
- ²¹S. Higashitaniguchi, M. Seto, S. Kitao, Y. Kobayashi, M. Saito, R. Masuda, T. Mitsui, Y. Yoda, Y. Kamihara, M. Hirano, and H. Hosono, *Phys. Rev. B* **78**, 174507 (2008).
- ²²K. Kitagawa, N. Katayama, K. Ohgushi, and M. Takigawa, *J. Phys. Soc. Jpn.* **78**, 063706 (2009).
- ²³R. Osborn, S. Rosenkranz, E. A. Goremychkin, and A. D. Christianson, *Physica C* **469**, 498 (2009).
- ²⁴We note that, intriguingly, scaling the resonance energy observed in the 122 compounds at 15 meV by T_C yields 23 meV.
- ²⁵A. N. Yaresko, G. Q. Liu, V. N. Antonov, and O. K. Andersen, *Phys. Rev. B* **79**, 144421 (2009).